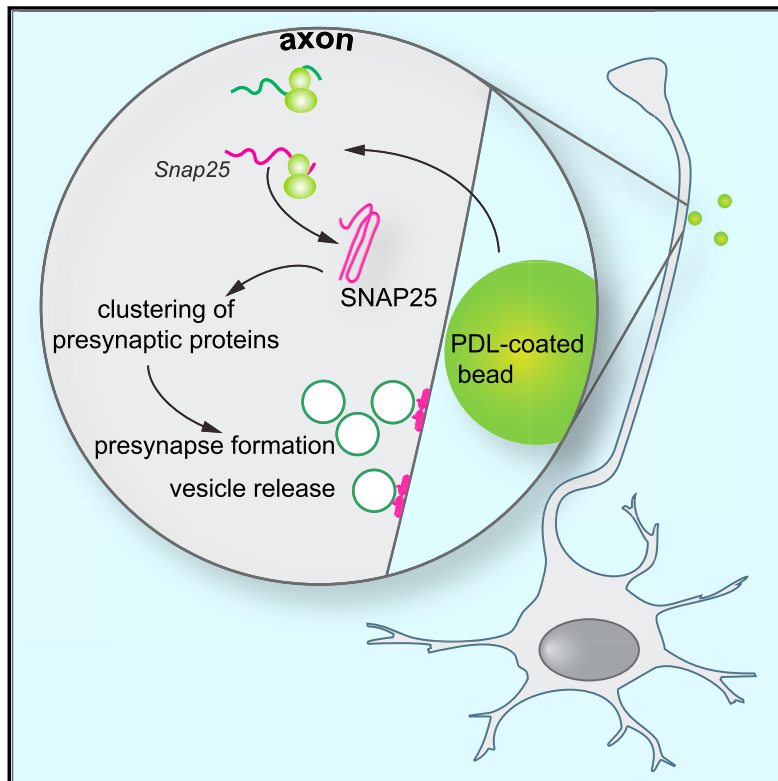


## Intra-axonal Synthesis of SNAP25 Is Required for the Formation of Presynaptic Terminals

### Graphical Abstract



### Authors

Andreia F.R. Batista, José C. Martínez, Ulrich Hengst

### Correspondence

uh2112@cumc.columbia.edu

### In Brief

Batista et al. find that, during the assembly of presynaptic terminals, mRNA translation is upregulated at the nascent presynapses and required for the clustering of presynaptic proteins. Inhibition of local SNAP25 synthesis prevents proper formation of presynaptic terminal and interferes with synaptic vesicle release.

### Highlights

- Protein synthesis is rapidly induced at contact sites with presynaptic organizers
- The presynaptic protein SNAP25 is locally synthesized at induced presynaptic sites
- Local SNAP25 synthesis is required for formation of presynapses
- Inhibition of local SNAP25 synthesis interferes with vesicle release



# Intra-axonal Synthesis of SNAP25 Is Required for the Formation of Presynaptic Terminals

Andreia F.R. Batista,<sup>1,2,3</sup> José C. Martínez,<sup>4</sup> and Ulrich Hengst<sup>3,5,\*</sup><sup>1</sup>Life and Health Sciences Research Institute (ICVS), School of Health Sciences, University of Minho, 4710-057 Braga, Portugal<sup>2</sup>ICVS/3B's, PT Associate Laboratory, Braga/Guimarães, Portugal<sup>3</sup>The Taub Institute for Research on Alzheimer's Disease and the Aging Brain and Department of Pathology & Cell Biology, Columbia University, New York, NY 10032, USA<sup>4</sup>Medical Scientist Training Program, Columbia University, New York, NY 10032, USA<sup>5</sup>Lead Contact\*Correspondence: [uh2112@cumc.columbia.edu](mailto:uh2112@cumc.columbia.edu)  
<http://dx.doi.org/10.1016/j.celrep.2017.08.097>

## SUMMARY

Localized protein synthesis is a mechanism for developing axons to react acutely and in a spatially restricted manner to extracellular signals. As such, it is important for many aspects of axonal development, but its role in the formation of presynapses remains poorly understood. We found that the induced assembly of presynaptic terminals required local protein synthesis. Newly synthesized proteins were detectable at nascent presynapses within 15 min of inducing synapse formation in isolated axons. The transcript for the t-SNARE protein SNAP25, which is required for the fusion of synaptic vesicles with the plasma membrane, was recruited to presynaptic sites and locally translated. Inhibition of intra-axonal SNAP25 synthesis affected the clustering of SNAP25 and other presynaptic proteins and interfered with the release of synaptic vesicles from presynaptic sites. This study reveals a critical role for the axonal synthesis of SNAP25 in the assembly of presynaptic terminals.

## INTRODUCTION

During the development of the nervous system, axons project over long distances to their cognate targets, until upon contact with target-derived adhesive or soluble factors the assembly of a presynaptic terminal is initiated (Chia et al., 2013; Jin and Garner, 2008). Application of these presynaptic organizing molecules to isolated axons is sufficient to induce presynapse formation from components that have been transported from the neuronal soma. An alternative source for at least some of the presynaptic proteins might be the axon itself through the process of local translation. Protein synthesis in axons is required for proper axon development (Campbell and Holt, 2001; Gracias et al., 2014; Hengst et al., 2009; Wu et al., 2005) by providing a spatially and temporally tightly restricted source of protein in response to extracellular signals (Batista and Hengst, 2016). Transcripts coding for several presynaptic proteins have been found in developing cortical axons (Taylor et al., 2009), and, in *Aplysia*, protein synthesis is required for

the formation of presynapses (Schacher and Wu, 2002). Recently, the importance of presynaptic protein synthesis in the control of neurotransmitter release was reported for the mature mammalian brain (Younts et al., 2016), but the role of local translation in the formation of presynapses remains poorly understood. Specifically, it is unknown whether axonal protein synthesis is required for the assembly of presynaptic terminals. So far, only one locally synthesized protein has been described that accumulates at nascent presynapses,  $\beta$ -catenin, where it regulates the release of synaptic vesicles (Taylor et al., 2013). Here, we report the induced intra-axonal synthesis of the t-SNARE protein synaptosomal-associated protein 25 (SNAP25) as a necessary, early step for the clustering of presynaptic proteins and the formation and function of presynapses.

## RESULTS

### Presynaptic Proteins Cluster within 1 hr at Contact Sites with PDL-Coated Beads

To investigate whether the formation of presynapses requires local protein synthesis, we cultured embryonic hippocampal neurons in tripartite microfluidic chambers that allow the fluidic isolation of axons from cell bodies and dendrites (Figure 1A) (Baleriola et al., 2014; Taylor et al., 2005). Poly-D-lysine (PDL)-coated latex beads were applied selectively to the axonal compartments to induce the clustering of presynaptic proteins (Lucido et al., 2009; Taylor et al., 2013). Immunostaining revealed significantly increased levels of several presynaptic proteins ( $\beta$ -catenin, synaptophysin, GAP-43, SNAP25) and tau at contact sites between axons and PDL-coated beads after 24 hr of incubation, while  $\beta$ -III tubulin levels were unchanged (Figure 1B). As local protein synthesis is frequently an acute reaction to an external stimulus, we next investigated how early after addition of the PDL-coated beads we could detect clustering of presynaptic proteins. SNAP25 levels were significantly increased after 1 hr of contact with the PDL-coated beads (Figure 1C).

### Inhibition of Axonal Protein Synthesis Prevents Clustering of $\beta$ -Catenin and SNAP25 at 1 hr

Previously, it has been reported that the clustering of  $\beta$ -catenin at 3 hr after addition of PDL-coated beads requires local protein synthesis (Taylor et al., 2013). To determine whether the clustering of other presynaptic proteins is likewise dependent on



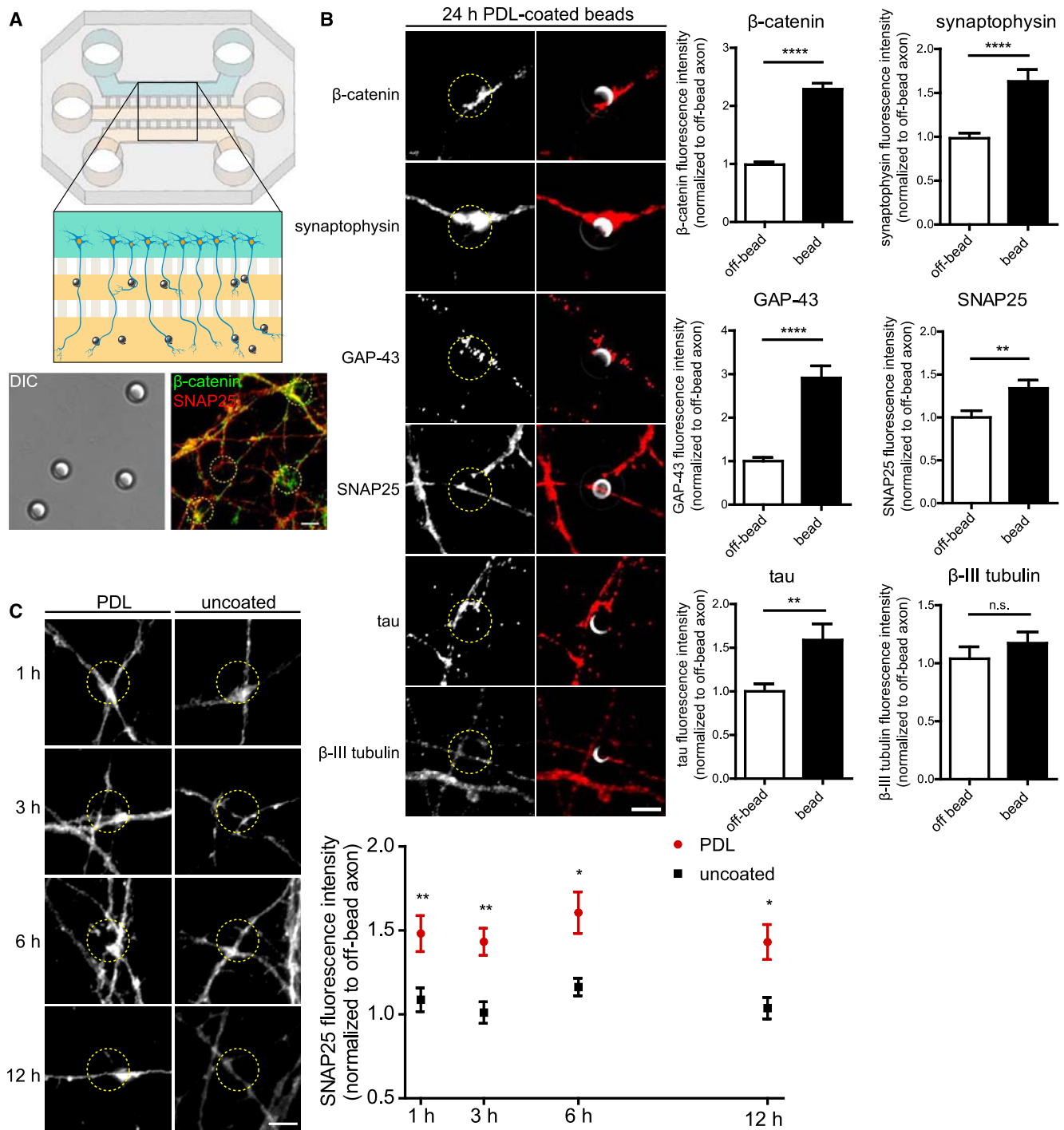


**Figure 1. Clustering of Presynaptic Markers at PDL-Coated Beads in Axons**

(A) Scheme of a tripartite microfluidic chamber used to selectively treat axons. Embryonic hippocampal neurons were seeded in the upper compartment of the chamber (teal) and axons cross through two microgroove barriers (500- $\mu$ m-long) into the middle and lower axonal compartments (yellow). After DIV10, PDL-coated or uncoated beads were added to the axonal compartments for 15 min to 1 hr, and clustering of presynaptic proteins (i.e.,  $\beta$ -catenin, SNAP25) adjacent to the bead-axon contact sites was determined by immunofluorescence (IF).

(B) Axons were incubated with PDL-coated beads for 24 hr and immunostained for presynaptic and axonal proteins. Levels of  $\beta$ -catenin, synaptophysin, SNAP25, GAP43, and tau are significantly increased at axon-bead contact sites. IF and IF merged with differential interference contrast (DIC) images are shown; yellow dashed circles outline beads. Quantifications are relative to off-bead fluorescence values. Mean  $\pm$  SEM of 30–120 axonal fields ( $n = 3$  biological replicates per condition). Unpaired t tests. n.s., not significant; \*\* $p < 0.01$ ; \*\*\*\* $p < 0.0001$ .

(legend continued on next page)

axonal translation, we focused on SNAP25 and added the protein synthesis inhibitor emetine selectively to the axonal compartment during the treatment with uncoated or PDL-coated beads (Figure 2A). We quantified the fluorescent intensity within axons along a 30- $\mu$ m-long line starting at the center of the beads (Figure 2B). Within 1 hr of treatment with PDL-coated beads,  $\beta$ -catenin and SNAP25 were significantly increased in the first 5  $\mu$ m from the beads' centers, i.e., at contact sites (Figures 2C–2E). The clustering of  $\beta$ -catenin and SNAP25 did not show any bias for either the proximal (i.e., toward the cell body) or distal side of the beads (Figure S1); thus, for our analyses we did not distinguish between the proximal and distal sides. Uncoated beads did not induce clustering, and addition of emetine completely prevented the clustering of  $\beta$ -catenin and SNAP25. Neither tau nor  $\beta$ -III tubulin clustered at this early time point (Figures 2F and 2G). To determine whether the observed protein synthesis dependency of  $\beta$ -catenin and SNAP25 clustering at 1 hr was limited to this early time point, we analyzed their clustering at 3, 6, and 12 hr after addition of beads and emetine to the axons. While SNAP25 clustering required protein synthesis at all time points tested,  $\beta$ -catenin clustering was significantly affected by emetine only at 3 hr (as previously reported by Taylor et al., 2013, but not at the later time points [Figure 2H]).

### PDL-Coated Beads Induce Protein Synthesis at Axonal Contact Sites within 15 min

The requirement for local translation for clustering after 1 hr of incubation with PDL-coated beads indicated that this treatment might trigger protein synthesis directly and acutely at contact sites with axons. We used puromycylation, also known as SUnSET (Figure 3A) (Schmidt et al., 2009), to detect protein synthesis events in axons. Puromycin is a tRNA analog that gets incorporated into the nascent protein chain (Yarmolinsky and Haba, 1959), allowing the detection of protein synthesis in situ with an anti-puromycin antibody. We detected a significant increase in the number of puromycin-positive puncta in axons at contact sites within 15 min of addition of PDL-coated beads (Figure 3B). The increase of the puromycin signal was accompanied by an increased presence of phospho-4EBP1, a marker for active translation, at contact sites with PDL-coated but not uncoated beads (Figure 3C). To investigate whether the immediate induction of protein synthesis was sustained over a longer time period, we added the beads for 1 hr and shifted the puromycylation time window to the last 10 min of the assay. As before, the addition of PDL-coated beads was associated with a significantly higher number of puromycylation-positive puncta in their immediate vicinity compared to uncoated beads, and addition of the protein synthesis inhibitor anisomycin completely abolished this effect (Figure 3D).

### Detection of SNAP25 mRNA in Axons by Fluorescent In Situ Hybridization

mRNA encoding SNAP25 has previously been found in axons of cortical neurons (Taylor et al., 2009), but it was below the detec-

tion threshold in other axonal transcriptome datasets (Baleriola et al., 2014; Zivraj et al., 2010). Here, we used single-molecule inexpensive fluorescent in situ hybridization (smiFISH; Tsanov et al., 2016) to directly visualize SNAP25 transcripts in axons of dissociated embryonic hippocampal neurons and to determine whether their intra-axonal localization changes in response to treatment with PDL-coated beads (Figure 4A). SNAP25 mRNA FISH-positive puncta were readily detectable at contact sites with PDL-coated beads, indicating that contact with PDL-coated beads recruits SNAP25 transcripts. The axonal smiFISH signal for SNAP25 mRNA was specific as transfection of axons with a SNAP25 small interfering RNA (siRNA) greatly reduced the number of positive puncta (Figure 4B).

### SNAP25 Is Synthesized Locally at Contact Sites of Axons with PDL-Coated Beads

The protein synthesis-dependent clustering of SNAP25 and the presence of its mRNA in axons at contact sites with PDL-coated beads indicated that SNAP25 itself might be locally produced. To test this hypothesis, we adopted a different design of microfluidic chambers (Figure 4C) (Park et al., 2009). In these circular chambers, axons grow into the central open compartment, allowing the collection of axonal material in quantities required for biochemistry. SNAP25 protein was detectable by immunoblot in lysates of axons treated with uncoated beads. Application of PDL-coated beads for 24 hr greatly increased the presence of SNAP25 in axons and treatment of axons with emetine reduced SNAP25 below detection limit without affecting SNAP25 expression in the cell body compartment (Figure 4C). To directly visualize SNAP25 synthesis at contact sites with PDL-coated beads, we combined puromycylation with a proximity ligation assay (puro-PLA) (Figure 4D) (tom Dieck et al., 2015). Axons that were not treated with PDL-coated beads showed very few SNAP25 puro-PLA puncta, while treatment with PDL-coated beads induced the local synthesis of SNAP25 (Figure 4E). As before, we tested how persistent the induction of SNAP25 synthesis was by incubating the axons for 1 hr with PDL-coated beads and adding puromycin for the last 10 min. SNAP25 puro-PLA puncta were readily detectable, and their presence was abolished by the presence of the protein synthesis inhibitor anisomycin (Figure 4F). Together, these results establish that SNAP25 is locally synthesized upon contact of axons with PDL-coated beads.

### SNAP25 Is Locally Synthesized at Synapses

So far, our approach has been to induce formation of presynapses by applying PDL-coated beads. This approach allows us to study presynaptic events required for the clustering of presynaptic proteins in the absence of a postsynaptic cell, but it is necessarily artificial. To test whether SNAP25 is locally synthesized at synapses rather than at induced presynaptic specializations, we cultured embryonic hippocampal neurons in regular dissociated cultures and performed SNAP25 puro-PLA assays on DIV5, 10,

(C) Axons were incubated with PDL-coated and uncoated beads for the indicated times and immunostained for SNAP25. SNAP25 immunoreactivity is significantly increased at contact sites with PDL-coated beads at all time points. Fluorescence is normalized to off-bead values. Mean  $\pm$  SEM of 30–50 axonal fields ( $n = 3$ –4 different biological replicates per condition). Two-way ANOVA with Bonferroni's multiple comparison test. \* $p < 0.05$ ; \*\* $p < 0.01$ . Scale bars, 5  $\mu$ m.

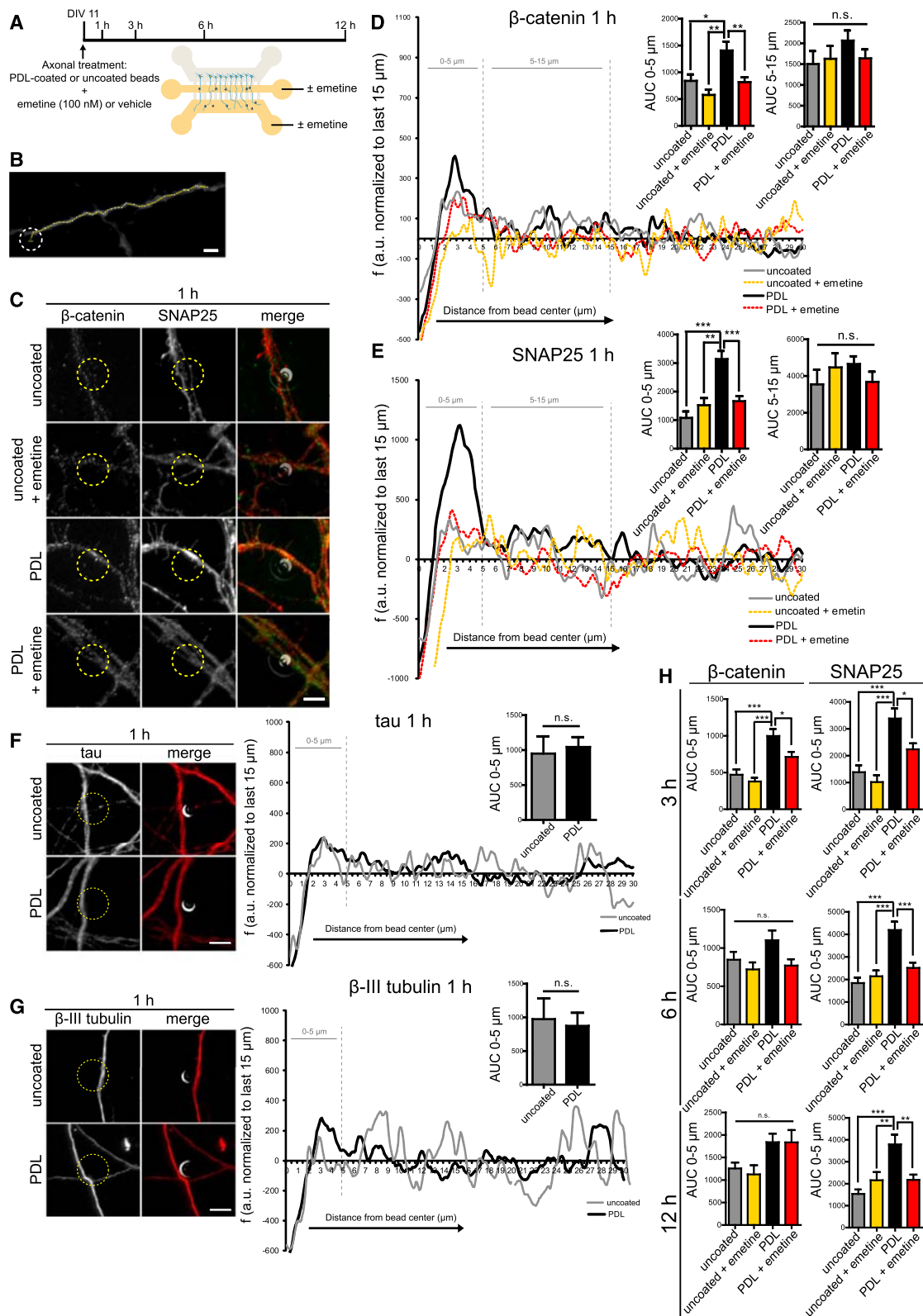


**Figure 2. Clustering of  $\beta$ -Catenin and SNAP25 at PDL-Coated Beads Requires Local Protein Synthesis**

(A) Experimental design: on DIV11 axons were treated with PDL-coated or uncoated beads in the presence of a protein synthesis inhibitor (emetine, 100 nM) or vehicle. Cultures were fixed at different time points after treatment.

(legend continued on next page)

and 15 (Figure 4G). SNAP25 puro-PLA puncta were visible in axons and dendrites at all developmental stages, and their frequency increased with the age of the cultures (Figure 4G). In DIV15 cultures, some SNAP25 puro-PLA puncta were found juxtapositioned to the postsynaptic protein PSD-95, indicating SNAP25 synthesis at established synapses. The appearance of SNAP25 puro-PLA puncta was prevented at all developmental stages if the cells were incubated with vehicle instead of puromycin or if the protein synthesis inhibitor anisomycin was added during the puromycylation (Figure 4H).

### Axon-Specific Knockdown of SNAP25 mRNA Reduces SNAP25 Synthesis at Contact Sites with PDL-Coated Beads

To investigate the requirement of localized SNAP25 or  $\beta$ -catenin mRNAs, we selectively transfected the axons of hippocampal neurons grown in microfluidic chambers with siRNA (Figure 5A). Previously, we have found that RNAi is functional in axons (Hengst et al., 2006) and that localized mRNAs can be selectively knocked down using locally applied siRNAs without affecting protein expression in dendrites or cell bodies (Baleriola et al., 2014; Gracias et al., 2014; Hengst et al., 2009; Villarin et al., 2016). When we transfected axons with a SNAP25 siRNA, the effect was restricted to axons (Figure 5B). The knockdown of SNAP25 mRNA in axons was only partial, likely because of the tight packaging of axonal mRNAs in granules (Buxbaum et al., 2014), which makes them inaccessible for the RNAi machinery while silenced but susceptible to siRNA under conditions that activate their translation, as we have observed previously (Baleriola et al., 2014; Villarin et al., 2016). Knockdown of axonal SNAP25 transcripts significantly reduced the appearance of SNAP25 puro-PLA puncta at contact sites with PDL-coated beads and increased that percentage of beads that had no puncta in their vicinity (Figure 5C). Together, these results establish that axonal transfection of SNAP25 siRNA is an efficient method to prevent the local translation of SNAP25 at contact sites with PDL-coated beads.

### Clustering of SNAP25 and $\beta$ -Catenin Requires the Presence of Their Transcripts in Axons

Next, we used this approach to investigate whether the local translation of SNAP25 or  $\beta$ -catenin was required for the clustering of these proteins. As before, we selectively knock down SNAP25 or  $\beta$ -catenin transcripts in axons by locally applied siRNA and measured protein clustering 1 hr after the application of PDL-coated beads (Figure 5D). Knockdown of axonal SNAP25 mRNA significantly prevented the clustering of SNAP25 at contact sites with PDL-coated beads (Figure 5E). Knockdown of  $\beta$ -catenin mRNA did not prevent clustering of

$\beta$ -catenin directly at the contact sites (0–5  $\mu$ m) but led to broadening of the peak with increased  $\beta$ -catenin levels at 5–10  $\mu$ m (Figure 5F). This result indicates that the vast majority of  $\beta$ -catenin protein clustering at PDL-coated beads is not derived from acutely triggered local synthesis but rather is of somatic origin. However, a small amount of  $\beta$ -catenin whose local synthesis is prevented by the siRNA appears to be required to induce the clustering of  $\beta$ -catenin directly at contact sites. The  $\beta$ -catenin siRNA used here efficiently knocks down its target mRNA when applied to dissociated hippocampal neurons (Figure 5G). Together, these results suggest that most of the SNAP25 required during the early stages of presynapse formation is derived from local protein synthesis.

### Clustering of SNAP25 and $\beta$ -Catenin Requires Each Other's Local Synthesis

Next, we used the same experimental approach to test the reciprocal requirement of SNAP25 and  $\beta$ -catenin synthesis for the clustering of these proteins. Clustering of  $\beta$ -catenin protein was significantly reduced in axons depleted of SNAP25 mRNA (Figure 6A). In axons with  $\beta$ -catenin mRNA knockdown, clustering of SNAP25 protein was reduced as well, and the peak for SNAP25 was broadened as we had seen before for  $\beta$ -catenin protein itself (Figure 6B).

### Knockdown of Axonal SNAP25 mRNA Interferes with Vesicle Release from Induced Presynaptic Sites

Last, we performed functional assays on induced presynaptic sites in axons transfected with siRNA similar to a previously described approach (Taylor et al., 2013). To study the release of synaptic vesicles at induced presynaptic sites, we used FM4-64. FM dyes are lipophilic dyes that can be endocytosed and incorporated into synaptic vesicles. We stimulated cells with a high potassium solution in the presence of FM4-64 and let dye endocytosis occur. Cells were then imaged and stimulated a second time with high potassium. As vesicles are exocytosed, dye molecules are released and rapidly diffuse, resulting in nerve terminal destaining. In axons transfected with the siRNA targeting SNAP25, release of synaptic vesicles as measured by the disappearance of fluorescence was significantly slower than in scrambled siRNA-transfected axons, while the loading was not different (Figures 7A and 7B). Again, this effect was limited to the siRNA-treated axons, as the unloading dynamic was unchanged at synapses in the cell body compartment (Figure 7C). As an additional control, we transfected axons with an siRNA targeting another presynaptic protein, piccolo (Fenster et al., 2000), whose transcript is absent from axonal transcriptome or translatome datasets (Shigeoka et al., 2016; Taylor et al., 2009).

(B) A three-pixel-wide line was drawn along the axon, starting at the center of the bead. Fluorescence along this line was quantified for 30  $\mu$ m and normalized against the average fluorescence in last 15  $\mu$ m. Beads have a diameter of 5  $\mu$ m.

(C–G) Axons were immunostained for  $\beta$ -catenin (C and D), SNAP25 (C and E), tau (F), and  $\beta$ -III tubulin (G) after 1 hr of treatment.  $\beta$ -catenin and SNAP25 increased in the direct vicinity of the beads in a protein synthesis inhibitor sensitive manner, while tau and  $\beta$ -III tubulin levels remained unchanged. IF and IF merged with DIC images are shown; yellow dashed circles outline beads. Fluorescence intensities obtained in the lines scans were averaged and normalized. The area under the curve (AUC) was then calculated for the first 5  $\mu$ m and 5–15  $\mu$ m from the bead center. Mean  $\pm$  SEM of 30–120 beads ( $n = 3$  biological replicates per condition).

(H) Axons were immunostained for  $\beta$ -catenin or SNAP25 after 3, 6, or 24 hr of treatment. SNAP25 levels were significantly increased at bead contact sites at all times tested. The effect for  $\beta$ -catenin was significant only at 3 hr, and emetine did not affect  $\beta$ -catenin levels at 24 hr. One-way ANOVA with Tukey's multiple comparison tests and unpaired t tests. n.s., not significant; \* $p < 0.05$ ; \*\* $p < 0.01$ ; \*\*\* $p < 0.001$ . Scale bars, 5  $\mu$ m. See also Figure S1.

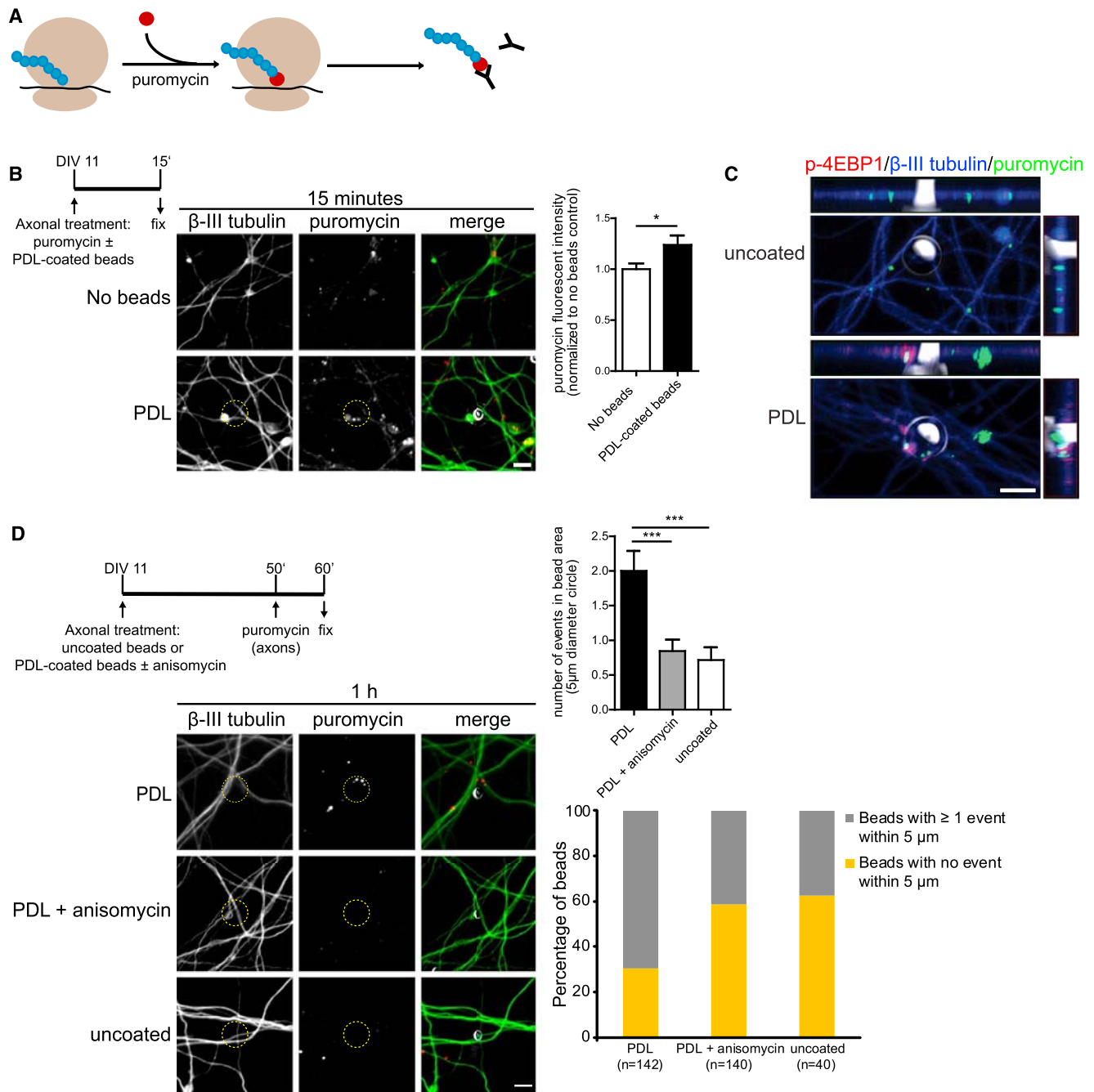


**Figure 3. PDL-Coated Beads Induce Axonal Protein Synthesis**

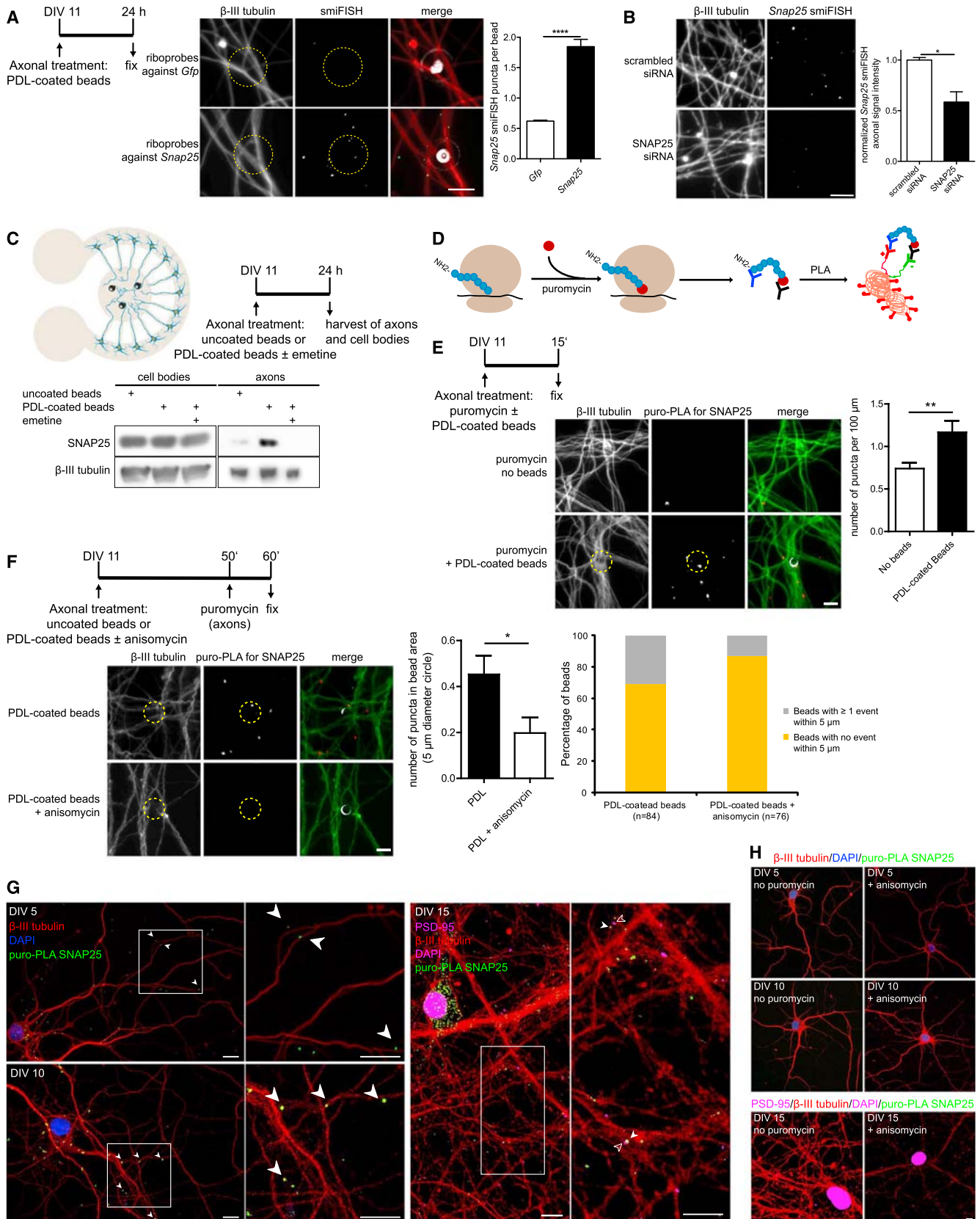
(A) Puromycylation assay: ribosomes incorporate puromycin into nascent polypeptide chains, leading to elongation termination and premature chain release. An antibody against puromycin is used to label nascent proteins in situ.

(B) Axons were treated with PDL-coated beads and puromycin or puromycin alone for 15 min and immunostained for puromycin and  $\beta$ -III tubulin. The level of puromycylation, indicating de novo protein synthesis is significantly increased at contact sites with PDL-coated beads. Mean  $\pm$  SEM of 30 axonal fields per condition ( $n = 3$  biological replicates). Unpaired t test. \* $p < 0.05$ .

(C) Axons were treated with uncoated or PDL-coated beads and puromycin for 15 min and immunostained for phospho-4EBP1,  $\beta$ -III tubulin, and puromycin. The signal for p-4EBP1, indicating activation of translation, co-localizes with the puromycin signal at contact sites with PDL-coated beads.

(D) Uncoated beads, PDL-coated beads, or PDL-coated beads and the protein synthesis inhibitor anisomycin (10  $\mu$ M) were added to the axonal compartments. Puromycin was added to axons during the last 10 min of the assay. The number of puromycin-positive puncta in a circle of 5  $\mu$ m around each bead center and the percentage of all beads imaged in each condition with no puncta or at least one puncta in the 5- $\mu$ m circle were plotted. Means  $\pm$  SEM of 40–142 beads in 30 axonal fields ( $n = 3$  different biological replicates). One-way ANOVA with Tukey's multiple comparison test. \* $p < 0.05$ ; \*\*\* $p < 0.001$ .

Yellow dashed line represents bead location. Scale bars, 5  $\mu$ m.



(legend on next page)



Neuron-wide knockdown of piccolo causes enhanced synaptic vesicles exocytosis rates (Leal-Ortiz et al., 2008), but axon-specific delivery of piccolo siRNA had no effect on synaptic vesicle release, again demonstrating that the siRNAs act only locally in axons and do not interfere with protein expression and transport from the cell body (Figure 7D).

## DISCUSSION

Our results establish that SNAP25 synthesis is locally activated by a presynaptic organizing signal and required for presynaptic terminal assembly. Previously, it has been reported that  $\beta$ -catenin is locally synthesized at nascent presynaptic sites and that the locally produced protein regulates the release dynamics of synaptic vesicles (Taylor et al., 2013). The question of whether local protein synthesis was required for the assembly of presynaptic terminal was not directly addressed. Here, we demonstrate that localized protein synthesis is a required step in the formation of presynaptic sites.

In accordance with Taylor et al. (2013), we also detect that  $\beta$ -catenin is locally synthesized. We find, however, differences in the requirement for local SNAP25 and  $\beta$ -catenin synthesis. While inhibition of protein synthesis prevents the accumulation of SNAP25 protein at contact sites with PDL-coated beads at all time points tested (1–12 hr), the accumulation of  $\beta$ -catenin is only affected until the 3-hr time point, indicating that at this time anterograde transport sufficiently meets the demand for  $\beta$ -catenin at presynapses. This difference is not easily explained by differences in the stability of SNAP25 and  $\beta$ -catenin: the half-life of SNAP25 during synaptogenesis in cerebellar granule neurons was reported to be 16 hr (Sanders et al., 1998), slightly longer than the half-life of  $\beta$ -catenin in PC12 cells of 12 hr (Bareiss et al., 2010). Instead, the role of the locally synthesized proteins

appears to differ. While axonal-specific siRNA treatment prevents the clustering of SNAP25 directly at contact sites with PDL-coated beads by around 50%, the analogous treatment leads to a broadening of the profile for  $\beta$ -catenin: the amount of protein found directly at beads is not significantly reduced but instead more  $\beta$ -catenin accumulates in the vicinity of the beads (5- to 15- $\mu$ m distance from the bead center). These findings indicate that 1 hr after contact with the beads nearly half of presynaptic SNAP25 protein is derived from local synthesis. In contrast, nearly all  $\beta$ -catenin accumulates at or near the beads independently of local protein synthesis, i.e., by anterograde transport from the cell body. The small amount of locally produced  $\beta$ -catenin is required to cluster the anterogradely transported protein directly at presynaptic sites. Thus, while local production of  $\beta$ -catenin is required only during the first steps of presynapse assembly and does not generate the bulk of presynaptic  $\beta$ -catenin protein, SNAP25 synthesis persists at least until 12 hr after initiation of presynapse formation, it generates a substantial amount of synaptic SNAP25 proteins, and it continues to be required even in established synapses, as demonstrated by the effect of axonal SNAP25 mRNA knockdown on synaptic vesicle release.

A recent translome analysis of retinal ganglion cells axons identified SNAP25 as highly expressed not only in developing, but also in mature axons (Shigeoka et al., 2016), and inhibition of protein synthesis at established presynaptic terminals deregulates GABA release (Younts et al., 2016). The stability of SNAP25 at presynapses is controlled by activity induced ubiquitination and proteasome-dependent degradation (Sheehan et al., 2016). SNAP25 synthesis at established synapses might therefore be an important mechanism for the control of synaptic SNAP25 levels and synapse function.

mRNA localization to axons is generally understood to be controlled by RNA-binding proteins that associated with mRNAs

### Figure 4. SNAP25 Is Locally Synthesized in Axons

(A) After DIV11, PDL-coated beads were added to the axonal compartments, and 24 hr later cells were fixed and processed for *Snap25* or *Gfp* smiFISH, and *Snap25* and *Gfp* positive puncta at bead contact sites were counted. SNAP25 transcripts accumulated at bead contact sites. Mean  $\pm$  SEM of ten axonal fields per condition ( $n = 3$  biological replicates). Unpaired t test. \*\*\*\* $p < 0.0001$ . Scale bar, 5  $\mu$ m.

(B) Hippocampal neurons were cultured in microfluidic chambers for 10 days. siRNA was applied only to the axonal compartments for 24 hr, and the neurons were processed for *Snap25* smiFISH. Axonal transfection with SNAP25 siRNA greatly reduced the number of SNAP25 puncta, establishing the specificity of the axonal *Snap25* smiFISH signal. Mean  $\pm$  SEM of ten axonal fields per condition. Unpaired t tests. \* $p < 0.05$ . Scale bar, 5  $\mu$ m.

(C) Scheme of a circular microfluidic chamber used for selective axonal treatments and protein isolation. Embryonic hippocampal neurons are seeded in the inner compartment and axons cross through a microgroove barrier (500- $\mu$ m-long) into an open circular (6-mm-diameter) compartment. After DIV11, uncoated beads or PDL-coated beads with or without emetine (100 nM) were added to the axonal compartment only, and 24 hr later proteins were obtained from both somatic and axonal compartments and analyzed for immunoblot blot. Selective treatment of axons with PDL-coated beads resulted in an increase of SNAP25 protein only in axons but not in cell bodies. This increase was blocked with local application of the protein synthesis inhibitor emetine.

(D) Principle of puo-PLA: puromycin is incorporated by active ribosomes into nascent polypeptide chains. A proximity ligation assay with antibodies against puromycin and the protein of interest—here: SNAP25—is used to detect synthesis of this protein.

(E) Axons of hippocampal neurons cultured in microfluidic chambers for 11 days were treated with PDL-coated beads and puromycin or puromycin alone for 15 min and processed for puo-PLA against SNAP25. The number of SNAP25 puo-PLA puncta is significantly increased in axons incubated with PDL-coated beads. Mean  $\pm$  SEM of ten axonal fields per condition ( $n = 3$  biological replicates). Unpaired t test. \*\* $p < 0.01$ .

(F) PDL-coated beads or PDL-coated beads and the protein synthesis inhibitor anisomycin (10  $\mu$ M) were added to the axonal compartments for 1 hr. Puromycin was added to axons during the last 10 min of the assay. The number of SNAP25 puo-PLA-positive puncta in a circle of 5  $\mu$ m around each bead center and the percentage of all beads imaged in each condition with no puncta or at least one puncta in the 5- $\mu$ m circle were plotted. Means  $\pm$  SEM of 76–84 beads in five to ten axonal fields per condition ( $n = 4$  different biological replicates). Scale bars, 5  $\mu$ m.

(G) Dissociated hippocampal neurons were cultured for 5, 10, or 15 days and incubated with puromycin for 10 min before fixation. Closed arrowheads indicate puo-PLA puncta and opened arrowheads PSD-95 puncta. Scale bars, 10  $\mu$ m.

(H) Dissociated hippocampal neurons were cultured for 5, 10, or 15 days and processed for SNAP25 puo-PLA without puromycin incubation or after incubation with puromycin and anisomycin for 10 min before fixation. Closed arrowheads indicate puo-PLA puncta and opened arrowheads PSD-95 puncta. Scale bars, 10  $\mu$ m.

See also Table S1.

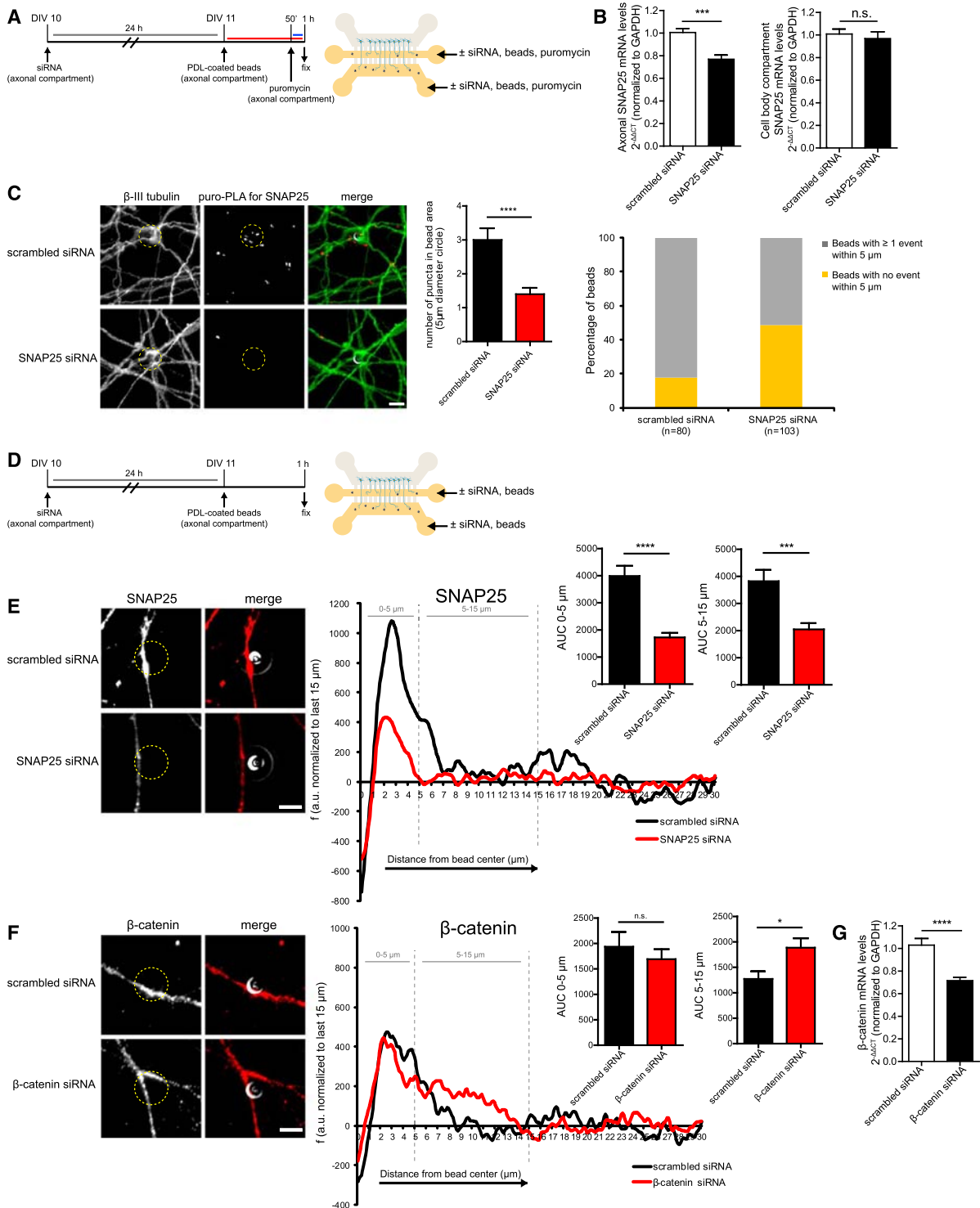


**Figure 5. Effect of Local siRNA on  $\beta$ -Catenin and SNAP25 Clustering**

(A) Experimental design for (C): hippocampal neurons were cultured in microfluidic chambers for 10 days. siRNA was applied only to the axonal compartments for 24 hr before PDL-coated beads were added for 1 hr. Puromycin was added to the axons for the last 10 min before fixation and processing for SNAP25 puro-PLA. (B) SNAP25 mRNA levels were quantified by RT-PCR in lysates obtained from the axonal and the cell body compartment 48 hr after transfection of the axons with siRNA. SNAP25 levels were significantly reduced in axons but not in the cell bodies, demonstrating that the axonally applied siRNAs act exclusively locally. Mean  $\pm$  SEM (n = 3 biological replicates).

(legend continued on next page)

through sequence elements nearly always found in the 3' UTRs of the transcripts. Interestingly, several SNPs located in the 3' UTR of SNAP25 are linked to adult attention deficit disorder (ADHD) (Barr et al., 2000; Brophy et al., 2002; Kustanovich et al., 2003; Mill et al., 2004). In the context of our findings, it is tempting to speculate that these mutations might interfere with the local synthesis of SNAP25 at presynaptic sites. Future investigation of the potentially changes in subcellular localization and synaptic translation of SNAP25 mRNA might provide a mechanistic understanding of how these mutations are linked to hyperactive disorders.

In conclusion, we describe an alternative source for presynaptic proteins, intra-axonal synthesis, that is required the formation presynaptic terminals.

## EXPERIMENTAL PROCEDURES

### Compartmentalized Culture of Embryonic Hippocampal Neurons

All work involving animals was performed in accordance with NIH guidelines for the care and use of laboratory animals and was approved by the Institutional Animal Use and Care Committee (IACUC) of Columbia University. All reagents were purchased from Thermo Fisher Scientific unless otherwise noted. Hippocampal neurons were harvested from Sprague-Dawley embryonic day 17/18 rat embryos (Kaech and Banker, 2006). Embryonic rat neurons were grown in tripartite microfluidic chambers with 500- $\mu\text{m}$ -long microgrooves connecting the three fluidically isolated compartments. Microfluidic chambers were produced according to published protocols (Gracias et al., 2014; Park et al., 2006). Primary hippocampal neurons (50,000–60,000 cells per chamber) were cultured in one of the side compartments, and axons were allowed to grow into the other two compartments. Chambers were coated with 0.1 mg mL<sup>-1</sup> poly- $\text{D}$ -lysine (Sigma-Aldrich) and 2  $\mu\text{g}$  mL<sup>-1</sup> laminin (Trevigen). After 24 hr, plating medium (neurobasal, 10% fetal bovine serum, 100 mM glutamine, 1 mM sodium pyruvate, 100 IU mL<sup>-1</sup> penicillin, 100  $\mu\text{g}$  mL<sup>-1</sup> streptomycin) was completely exchanged for growth medium (neurobasal, 1  $\times$  B27, 100 mM glutamine). Half of this growth medium was replaced with fresh growth medium on DIV4 and 8. All experiments were performed at DIV9–11. Whenever stated, axonal compartments were treated with emetine (100 nM, EMD Millipore) or anisomycin (10  $\mu\text{M}$ , Sigma-Aldrich).

### Presynaptic Clustering with PDL-Coated Beads

Bead preparation and treatments were performed as described (Lucido et al., 2009; Taylor et al., 2013). Surfactant-free aliphatic amine latex microspheres 4–5  $\mu\text{m}$  in diameter (Invitrogen) were coated in 50  $\mu\text{g}$  mL<sup>-1</sup> PDL (Sigma-Aldrich) at 37°C for at least 2 hr, rinsed twice with water, and diluted in growth medium. Uncoated beads were incubated in water. Around 150,000 PDL-coated beads were added to each axonal compartment through the side access ports. As adhesion of uncoated beads to axons is much lower for uncoated than for PDL-coated beads they were added at five to ten times excess.

### Immunofluorescence and Line Scans

Neurons grown in microfluidic chambers were treated on DIV9–11 and fixed for 20 min at room temperature in 4% paraformaldehyde (PFA) in cytoskeleton

buffer (10 mM 2-(N-morpholino)ethanesulfonic acid [MES], 3 mM MgCl<sub>2</sub>, 138 mM KCl, 2 mM EGTA, 0.32 M sucrose [pH 6.1]). Neurons were washed with PBS, permeabilized, and blocked for 30 min with 3 mg mL<sup>-1</sup> BSA, 100 mM glycine, and 0.25% Triton X-100. Coverslips were incubated overnight at 4°C with primary antibodies: rabbit anti- $\beta$ -catenin (1:500, Invitrogen, 71-2700), mouse anti-synaptophysin (1:500, BioLegend, SY38), mouse anti-GAP-43 (1:500, Invitrogen, 7B10), mouse anti-SNAP25 (1:1,000, BioLegend, SMI 81), rabbit anti-tau (1:500, GenScript, phospho-Ser<sup>235</sup>), rabbit anti- $\beta$ III-tubulin (1:1,000, BioLegend, Poly18020), and mouse anti- $\beta$ III-tubulin (1:500, Abcam, TU-20). Neurons were washed with PBS and incubated with fluorophore-conjugated Alexa secondary antibodies (1:200) for 1 hr at room temperature. Samples were mounted with ProLong Diamond Antifade (Invitrogen), and images were acquired in z stacks using a 63 $\times$ /1.3 oil objective on an Axio-Observer.Z1 microscope equipped with an AxioCam MRm Rev. 3 camera (Zeiss). Acquisition settings were kept the same for all samples in any given experiment. Five random axonal fields containing beads were imaged per coverslip. To quantify average fluorescence intensity at axon-beads contact sites, a 5- $\mu\text{m}$ -diameter circle around the bead center was drawn in AxioVision, and average pixel intensity was determined inside that circle. For off-bead values, average pixel intensity was determined in a 5- $\mu\text{m}$  circle that encompassed axons not in proximity with beads. For each image, background fluorescence intensity was determined in an area with no axons and subtracted from all bead and off-bead values. To quantify fluorescence along the axons, starting at the center of the bead, a three-pixel-wide line was drawn along the axon using ImageJ. Average pixel intensity in that line was determined for 30  $\mu\text{m}$ . The intensity along the last 15  $\mu\text{m}$  of each segment was averaged, and the resulting off-bead mean axonal fluorescence intensity was subtracted from all values.

### Immunoblot Analysis

Hippocampal neurons were culture in circular microfluidic chambers modified after Park et al. (2009), in which the axon grows across a 500- $\mu\text{m}$ -long microgroove barrier into the inner open compartment (6 mm diameter). For protein isolation, medium was carefully removed from axonal compartment, and axons were collected in 50  $\mu\text{L}$  of RIPA buffer (50 mM Tris-HCl [pH 7.4], 150 mM NaCl, 0.25% deoxycholic acid, 1% NP-40, 1% SDS, 1 mM EDTA, supplemented with protease and phosphatase inhibitors [Pierce]), the chamber was then removed, and somatic material was collected in 100  $\mu\text{L}$  of RIPA buffer. The material from six different chambers was collected this way using the same buffer to increase the amount of protein. 20  $\mu\text{L}$  of lysate from axons and 2  $\mu\text{L}$  of lysate from cell bodies were used for western blotting. Nitrocellulose membrane was incubated with anti-SNAP-25 (1:1,000, BioLegend, 836304) or anti- $\beta$ -III tubulin (1:10,000, BioLegend, 802001) at 4°C overnight in TBS-T with 4% milk. For detection, blots were incubated with respective secondary antibodies (1:10,000, anti-Ms-horseradish peroxidase [HRP] or anti-Rb-HRP, Invitrogen) and developed with 1-Shot Digital-ECL (KindleBio, R1003), and images were taken with the KwikQuant Imager (KindleBio, D1001).

### Puromycylation and Puromycylation-Proximity Ligation Assays

To detect newly synthesized proteins, puromycin (1.8  $\mu\text{M}$ , Sigma-Aldrich) or growth medium was added to axons in compartmentalized cultures or to dissociated neurons in regular cultures for 10–15 min, depending on the experiment, in the absence or presence of the protein synthesis inhibitor anisomycin (10  $\mu\text{M}$  for axons, 40  $\mu\text{M}$  for dissociated cultures). After incubation, cells were

(C) Transfection of axons with SNAP25 siRNA greatly reduced the synthesis of SNAP25 at contact sites with PDL-coated beads as measured with SNAP25 puromycin (PURO). Mean  $\pm$  SEM of 80–103 beads in ten axonal fields per condition (n = 3 biological replicates).

(D) Experimental design for (E) and (F): hippocampal neurons were cultured and their axons selectively transfected with siRNAs and incubated with PDL-coated beads as in (A). The neurons were fixed after 1 hr and immunostained for SNAP25 (E) or  $\beta$ -catenin (F).

(E) SNAP25 immunostaining in the direct vicinity of PDL-coated beads is significantly reduced in axons transfected with SNAP25 siRNA. Average fluorescence values for 30  $\mu\text{m}$  from the bead center, and the mean AUC for the 0- to 5- $\mu\text{m}$  and 5- to 15- $\mu\text{m}$  regions are plotted.

(F)  $\beta$ -catenin immunostaining in the 0- to 5- $\mu\text{m}$  region is not significantly decreased in axons transfected with  $\beta$ -catenin siRNA. The signal intensity is increased in the 5- to 15- $\mu\text{m}$  region. Mean  $\pm$  SEM of 80–100 beads (n = 3 biological replicates).

(G) Dissociated hippocampal neurons were cultured for 11 days and transfected with siRNA, and  $\beta$ -catenin mRNA levels were determined by RT-PCR after 48 hr. Unpaired t tests. n.s., not significant; \*p < 0.05; \*\*\*p < 0.001; \*\*\*\*p < 0.0001. Yellow dashed lines represent bead outline. Scale bars, 5  $\mu\text{m}$ .

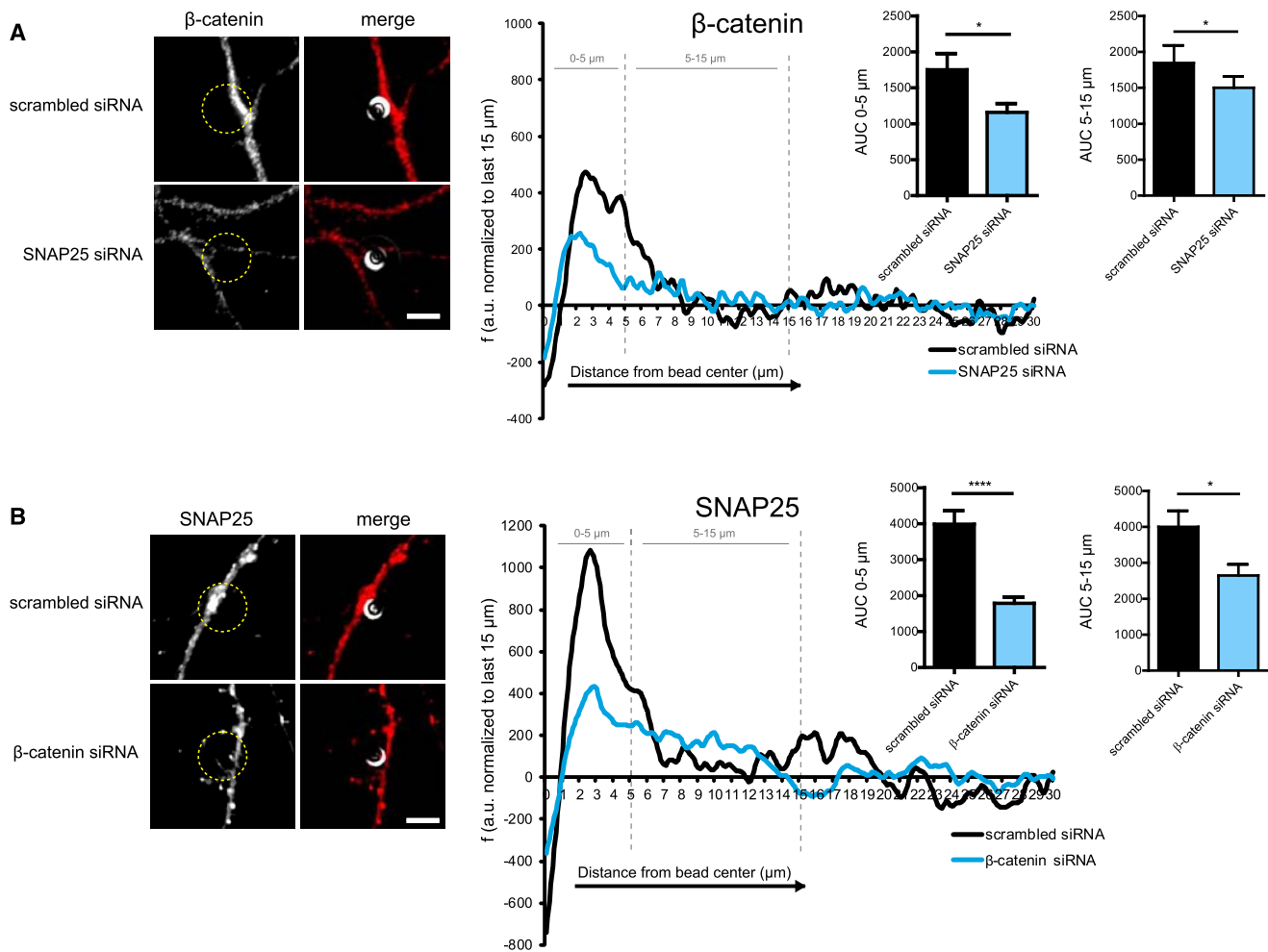


**Figure 6. Reciprocal Effects of Local β-Catenin and SNAP25 Knockdown on Clustering**

Hippocampal neurons were cultured and treated as in Figure 5D.

(A) Axons were transfected with scrambled or SNAP25 siRNA. 24 hr later, PDL-coated beads were added for 1 hr, and β-catenin clustering was determined by IF. Fluorescence values were quantified for 30 μm starting at the bead center and mean AUC for the 0- to 5-μm and 5- to 15-μm regions are plotted.

(B) Axons were transfected with scrambled or β-catenin siRNA. 24 hr later, PDL-coated beads were added for 1 hr, and SNAP25 clustering was determined by IF. Fluorescence values were quantified for 30 μm starting at the bead center and mean AUC for the 0- to 5-μm and 5- to 15-μm regions are plotted.

Mean ± SEM of 80–100 beads (n = of 3 different biological replicates). Unpaired t test. \*p < 0.05 \*\*\*\*p < 0.0001. Yellow dashed lines represent bead outline. Scale bars, 5 μm.

washed twice with warm PBS and fixed for 20 min at room temperature in 4% PFA in cytoskeleton buffer. Cells were washed with PBS, blocked, and permeabilized in 3 mg mL<sup>-1</sup> BSA, 100 mM glycine, and 0.25% Triton X-100 and incubated overnight at 4°C with mouse anti-puromycin antibody (1:250, Millipore, MABE343) and rabbit anti-SNAP25 antibody (1:250, Sigma-Aldrich, S9684) for the puro-PLA assay. Detection of newly synthesized SNAP25 through PLA was performed according to the manufacturer's recommendations, using rabbit PLA<sup>plus</sup> and mouse PLA<sup>minus</sup> probes and red Duolink detection reagents (Sigma-Aldrich). Before mounting with Duolink In Situ Mounting Medium with DAPI (Sigma-Aldrich), coverslips were incubated with anti-βIII-tubulin (1:100, Abcam, 2G10; conjugated to Alexa Fluor 488) or anti-βIII-tubulin (1:100, Abcam, EP1569Y; Alexa Fluor 647) and anti-PSD-95 (1:50, Abcam, EP2652Y; Alexa Fluor 488) for 1 hr at room temperature. Images were acquired as described previously and quantified by counting the number of puromycin-positive or PLA puncta. SNAP25 puro-PLA experiments in dissociated cultures were imaged in a Zeiss LSM 800 confocal microscope using a 40× oil objective and Zen Blue 2.1 software.

#### Single-Molecule Inexpensive Fluorescence In Situ Hybridization

Oligonucleotide probes were designed using Oligostan software (Tsanov et al., 2016). For *Snap25*, we obtained 30 probes, while for *Egfp* we designed 15 probes due to the smaller coding sequence (Table S1). The probes were hybridized to a digoxigenin-labeled FLAP oligonucleotide to create FLAP-structured duplex probes (Tsanov et al., 2016). smiFISH was performed as described (Tsanov et al., 2016), with minor changes. On DIV10, beads were added to the axonal compartments of hippocampal neurons grown in microfluidic devices. Cells were fixed after 24 hr for 20 min in 4% PFA in cytoskeleton buffer. Coverslips were washed in PBS, permeabilized with 0.3% Triton X-100 in PBS for 5 min, and washed again with PBS. Coverslips were equilibrated at 37°C in 15% formamide, 1 × saline sodium citrate (SSC). Samples were incubated with 10 pmol of FLAP-structured duplex probes in 50 μL of hybridization buffer (15% formamide, 1 × SSC, 10% dextran, 350 ng μL<sup>-1</sup> yeast tRNA, 0.2 mg mL<sup>-1</sup> BSA, 2 mM vanadyl ribonucleoside complex) overnight at 37°C. Coverslips were washed twice with 15% formamide in 1 × SSC for 30 min at 37°C. Afterward samples were washed three times with PBS-T

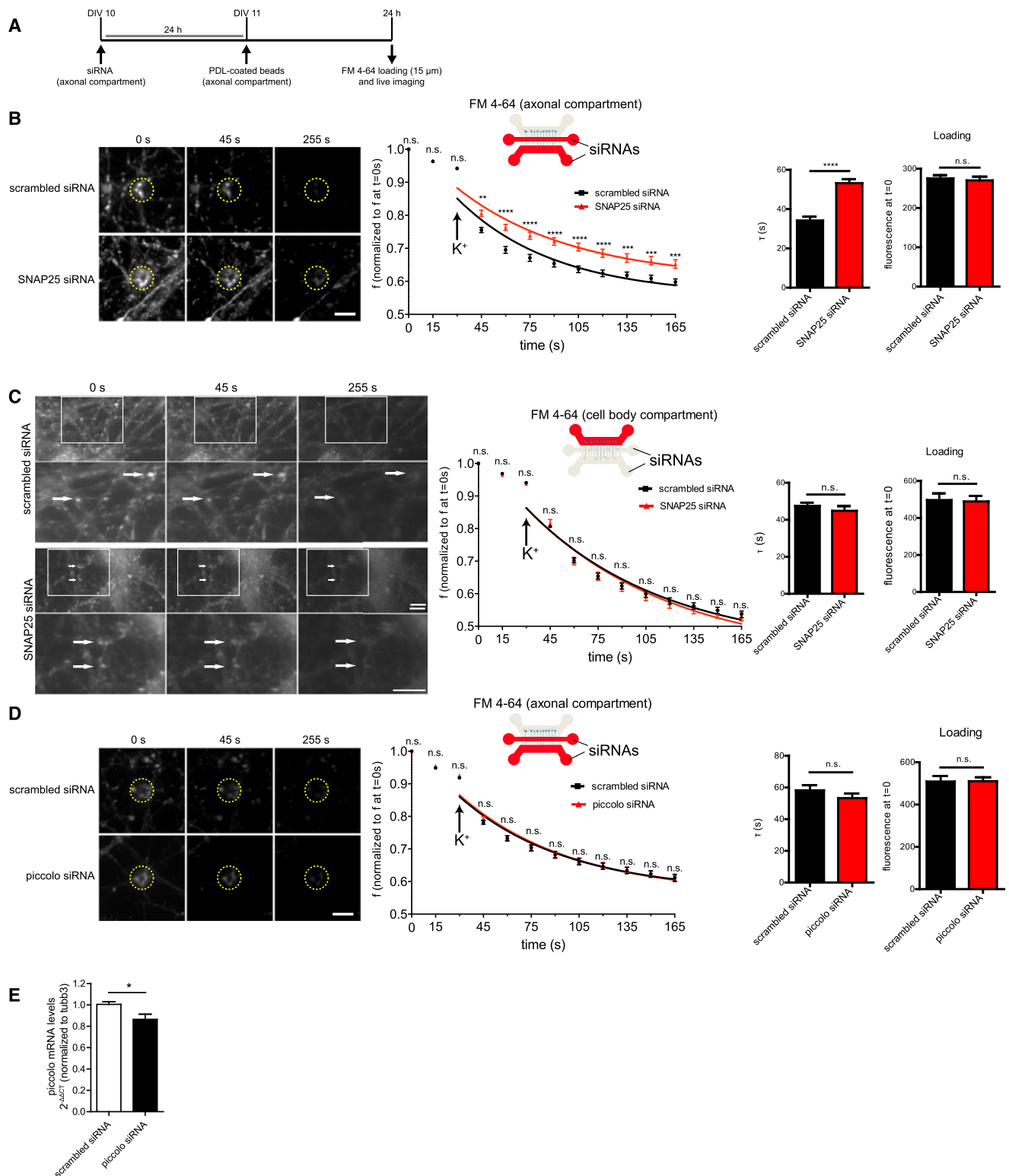


**Figure 7. Knockdown of Axonal SNAP25 mRNA Affects Vesicle Release of Newly Formed Synaptic Terminals**

(A) Experimental design: hippocampal neurons were cultured in microfluidic chambers for 10 days. Axons were transfected with siRNAs 24 hr before adding PDL-coated beads. 24 hr after bead incubation, cells were loaded with FM dyes and imaged.

(B) Sequential imaging and stimulation of FM4-64 puncta in scrambled or SNAP25 siRNA-treated axons at contact sites with PDL-coated beads. SNAP25 siRNA slows vesicle release after stimulation with potassium but does not impede FM4-64 loading. Pictures were taken every 15 s, high potassium was added after 30 s

(legend continued on next page)

(0.1% Tween 20) for 5 min, blocked with 3% BSA in PBS-T for 30 min, and incubated with goat anti-digoxigenin (1:500, Vector Laboratories) overnight at 4°C. Samples were washed three times with PBS-T for 5 min and incubated with Alexa 488 anti-goat secondary (1:1,000), and anti- $\beta$ -tubulin was conjugated to Alexa-594 (Abcam, ab201740) for 1 hr at room temperature. They were then washed with PBS and mounted with ProLong Diamond Antifade Mountant (Invitrogen). *Egfp* fluorescence was used as a control for nonspecific hybridization and subtracted from all *Snap25* values. The specificity of the *Egfp* probes was verified by performing smiFISH on cells transfected by a *Gfp* plasmid or control (data not shown). The specificity of the *Snap25* probe was verified by RNAi in axons (Figure 4B).

### siRNA Transfections

Axon-specific silencing of *Snap25*, *ctnnb1*, and *pcl* mRNAs was achieved using the following siRNAs: *Snap25* (NM\_001270575.1) 5'-CGUGUCGAA GAAGGGAUGAACCAUA-3' and 5'-UAUGGUUCAUGCCUUCUUCGACACG-3'; *ctnnb1* (NM\_053357.2) 5'-UCUGCAUGCCCUCUAGUGUCUC-3' and 5'-GAGGUCGAGAAGGCAUGAACCAUA-3'; and *pcl* (NM\_020098.1) 5'-CACCUUGCUGGUCUCACAUUAUU-3' and 5'-AAUAAUGAGAGACCA GCAAGGUG-3'. Negative control siRNA was purchased from Thermo Fisher Scientific (Stealth RNAi siRNA Negative Control Med GC Duplex #3). siRNAs were transfected into axons of DIV10 neurons grown in microfluidic chambers using NeuroPORTER transfection reagent (Genlantis). Final siRNA concentration was 50 nM. Beads were added 24 hr after transfection.

### Real-Time RT-PCR

Total RNA from cell bodies (four chambers or 150,000 cells) and axonal compartments (from a minimum of six chambers) was extracted with TRIzol, and RNA was purified using the Direct-zol RNA MiniPrep kit (Zymo Research). Axonal RNA was eluted in 10  $\mu$ L of nuclease-free water and reverse transcribed to cDNA using the Superscript VILO cDNA synthesis kit. For cell body RNA, a total of 100 ng was reverse transcribed to cDNA. Axonal cDNA was preamplified using the TaqMan PreAmp kit, following manufacturer's instructions for the 14 cycles preamplification. Real-time RT-PCR was performed with TaqMan Fast Advanced master mix in a StepOnePlus Real-Time PCR instrument, using pre-designed TaqMan probes. Amplification conditions were as follows: initial denaturing step at 95°C for 10 min, 40 cycles of denaturation at 95°C for 15 s, and extension at 60°C for 1 min. *Snap25*, *ctnnb1*, and *pcl* levels were normalized to *gapdh*.

### FM4-64 Release Assay

After DIV11, the chamber medium was exchanged with Tyrode's solution (125 mM NaCl, 2 mM KCl, 2 mM CaCl<sub>2</sub>, 2 mM MgCl<sub>2</sub>, 30 mM glucose, 25 mM HEPES [pH 7.4]), and cells were allowed to equilibrate for at least 30 min. Then, FM4-64 (15  $\mu$ M, N-[3-Triethylammoniumpropyl]-4-[6-[4-(Diethylamino) Phenyl] Hexatrienyl] Pyridinium Dibromide; Invitrogen) was loaded for 90 s in a high K<sup>+</sup> solution (37 mM NaCl, 90 mM KCl, 2 mM CaCl<sub>2</sub>, 2 mM MgCl<sub>2</sub>, 30 mM glucose, 25 mM HEPES [pH 7.4]) with 10  $\mu$ M CNQX (6-Cyano-7-nitroquinoxaline-2,3-dione disodium; Santa Cruz Biotechnology) and 50  $\mu$ M DL-AP5 (DL-2-Amino-5-phosphonovaleric acid, Santa Cruz Biotechnology). Cells were loaded for 10 more min in Tyrode's solution with FM4-64, CNQX, and DL-AP5. Chambers were then briefly washed twice in low Ca<sup>2+</sup> solution (112 mM NaCl, 2 mM KCl, 0.5 mM CaCl<sub>2</sub>, 10 mM MgCl<sub>2</sub>, 30 mM glucose, 25 mM HEPES

[pH 7.4]) with 0.5 mM advasep-7 (Sigma-Aldrich), CNQX, and DL-AP5 and three times in Tyrode's solution with CNQX and DL-AP5. Unloading was then evoked with high K<sup>+</sup> solution. During imaging, neurons were kept in a CO<sub>2</sub> and humidity controlled incubation chamber at 37°C. Images were acquired every 15 s, for a total of 4 min. High K<sup>+</sup> was added after 30 s. The intensity of FM4-64 puncta around beads was quantified over time. Relative fluorescence values were plotted and entered in SPSS (IBM). A monoexponential fit was calculated for each individual bead data with the equation,  $F = F_{max} \times e^{-time/\tau} + F_{final}$ , with  $F_{max}$  being the fluorescence value right before K<sup>+</sup> stimulation,  $\tau$  the exponential decay constant, and  $F_{final}$  the final plateau.  $\tau$  values were plotted and compared between conditions.

### Statistical Methods

Statistical analysis was performed using Prism 7 (GraphPad). The means of two groups were compared with unpaired t tests, and the means of three groups were compared using ANOVA with Tukey's multiple comparison test. The means of multiple groups with two independent variables were compared using two-way ANOVA with Bonferroni's multiple comparisons tests.

### SUPPLEMENTAL INFORMATION

Supplemental Information includes one figure and one table and can be found with this article online at <http://dx.doi.org/10.1016/j.celrep.2017.08.097>.

### AUTHOR CONTRIBUTIONS

A.F.R.B. and U.H. designed the experiments. A.F.R.B. and J.C.M. performed the experiments and data analysis. A.F.R.B. and U.H. wrote the paper.

### ACKNOWLEDGMENTS

A.F.R.B. was supported by the Portuguese Foundation for Science and Technology (FCT) in the context of the FCT funded University of Minho MD/PhD Program (SFRH/BD/52322/2013). J.C.M. was supported by the National Institutes of Health (F31GM116617). U.H. was supported by the NIH (R01MH096702), the BrightFocus Foundation (A2015093S), and the Irma T. Hirschl Trust.

Received: June 8, 2017

Revised: August 8, 2017

Accepted: August 29, 2017

Published: September 26, 2017

### REFERENCES

- Baleriola, J., Walker, C.A., Jean, Y.Y., Cray, J.F., Troy, C.M., Nagy, P.L., and Hengst, U. (2014). Axonally synthesized ATF4 transmits a neurodegenerative signal across brain regions. *Cell* 158, 1159–1172.
- Bareiss, S., Kim, K., and Lu, Q. (2010). Delta-catenin/NPRAP: A new member of the glycogen synthase kinase-3beta signaling complex that promotes beta-catenin turnover in neurons. *J. Neurosci. Res.* 88, 2350–2363.
- Barr, C.L., Feng, Y., Wigg, K., Bloom, S., Roberts, W., Malone, M., Schachar, R., Tannock, R., and Kennedy, J.L. (2000). Identification of DNA variants in the

(black arrow), and axons were imaged for 3.5 min more. Fluorescence at PDL-coated beads (yellow dashed circle) was quantified over time, and mean fluorescence, normalized to initial FM4-64 intensity, is shown with fitted exponential decay curves. The exponential destaining time constant ( $\tau$ ) for each bead and initial fluorescence values are plotted.

(C) FM4-64 puncta (white arrows) of neurites in the cell body compartment of chambers where siRNA was applied only to axons were also stimulated and imaged. Knockdown of *Snap25* mRNA in axons does not affect vesicle dynamics in the cell body compartment. Exponential decay time constant ( $\tau$ ) and initial fluorescence are shown.

(D) Neurons were treated as in (A) but their axons were transfected with a piccolo siRNA. The piccolo siRNA does not change axonal vesicle dynamics. Mean fluorescence at beads over time with fitted exponential decay curves, exponential decay constant ( $\tau$ ), and initial fluorescence are represented.

Mean  $\pm$  SEM of 45 beads per condition ( $n = 3$  different biological replicates). Decay plots: two-way ANOVA with multiple comparison test. Bar graphs: unpaired t tests. n.s., not significant; \*\* $p < 0.01$ ; \*\*\* $p < 0.001$ ; \*\*\*\* $p < 0.0001$ ; p < 0.001. Scale bars, 5  $\mu$ m.

(E) Dissociated hippocampal neurons were cultured for 11 days and transfected with siRNA, and piccolo mRNA levels were determined by RT-PCR after 48 hr. Mean  $\pm$  SEM ( $n = 3$  different biological replicates). Unpaired t test. \* $p < 0.05$ .

- SNAP-25 gene and linkage study of these polymorphisms and attention-deficit hyperactivity disorder. *Mol. Psychiatry* 5, 405–409.
- Batista, A.F., and Hengst, U. (2016). Intra-axonal protein synthesis in development and beyond. *Int. J. Dev. Neurosci.* 55, 140–149.
- Brophy, K., Hawi, Z., Kirley, A., Fitzgerald, M., and Gill, M. (2002). Synaptosomal-associated protein 25 (SNAP-25) and attention deficit hyperactivity disorder (ADHD): Evidence of linkage and association in the Irish population. *Mol. Psychiatry* 7, 913–917.
- Buxbaum, A.R., Wu, B., and Singer, R.H. (2014). Single  $\beta$ -actin mRNA detection in neurons reveals a mechanism for regulating its translatability. *Science* 343, 419–422.
- Campbell, D.S., and Holt, C.E. (2001). Chemotropic responses of retinal growth cones mediated by rapid local protein synthesis and degradation. *Neuron* 32, 1013–1026.
- Chia, P.H., Li, P., and Shen, K. (2013). Cell biology in neuroscience: Cellular and molecular mechanisms underlying presynapse formation. *J. Cell Biol.* 203, 11–22.
- Fenster, S.D., Chung, W.J., Zhai, R., Cases-Langhoff, C., Voss, B., Garner, A.M., Kaempf, U., Kindler, S., Gundelfinger, E.D., and Garner, C.C. (2000). Piccolo, a presynaptic zinc finger protein structurally related to bassoon. *Neuron* 25, 203–214.
- Gracias, N.G., Shirkey-Son, N.J., and Hengst, U. (2014). Local translation of TC10 is required for membrane expansion during axon outgrowth. *Nat. Commun.* 5, 3506.
- Hengst, U., Cox, L.J., Macosko, E.Z., and Jaffrey, S.R. (2006). Functional and selective RNA interference in developing axons and growth cones. *J. Neurosci.* 26, 5727–5732.
- Hengst, U., Deglincerti, A., Kim, H.J., Jeon, N.L., and Jaffrey, S.R. (2009). Axonal elongation triggered by stimulus-induced local translation of a polarity complex protein. *Nat. Cell Biol.* 11, 1024–1030.
- Jin, Y., and Garner, C.C. (2008). Molecular mechanisms of presynaptic differentiation. *Annu. Rev. Cell Dev. Biol.* 24, 237–262.
- Kaech, S., and Banker, G. (2006). Culturing hippocampal neurons. *Nat. Protoc.* 1, 2406–2415.
- Kustanovich, V., Merriman, B., McGough, J., McCracken, J.T., Smalley, S.L., and Nelson, S.F. (2003). Biased paternal transmission of SNAP-25 risk alleles in attention-deficit hyperactivity disorder. *Mol. Psychiatry* 8, 309–315.
- Leal-Ortiz, S., Waites, C.L., Terry-Lorenzo, R., Zamorano, P., Gundelfinger, E.D., and Garner, C.C. (2008). Piccolo modulation of Synapsin1a dynamics regulates synaptic vesicle exocytosis. *J. Cell Biol.* 181, 831–846.
- Lucido, A.L., Suarez Sanchez, F., Thostrup, P., Kwiatkowski, A.V., Leal-Ortiz, S., Gopalakrishnan, G., Liazoghli, D., Belkaid, W., Lennox, R.B., Grutter, P., et al. (2009). Rapid assembly of functional presynaptic boutons triggered by adhesive contacts. *J. Neurosci.* 29, 12449–12466.
- Mill, J., Richards, S., Knight, J., Curran, S., Taylor, E., and Asherson, P. (2004). Haplotype analysis of SNAP-25 suggests a role in the aetiology of ADHD. *Mol. Psychiatry* 9, 801–810.
- Park, J.W., Vahidi, B., Taylor, A.M., Rhee, S.W., and Jeon, N.L. (2006). Microfluidic culture platform for neuroscience research. *Nat. Protoc.* 1, 2128–2136.
- Park, J., Koito, H., Li, J., and Han, A. (2009). Microfluidic compartmentalized co-culture platform for CNS axon myelination research. *Biomed. Microdevices* 11, 1145–1153.
- Sanders, J.D., Yang, Y., and Liu, Y. (1998). Differential turnover of syntaxin and SNAP-25 during synaptogenesis in cultured cerebellar granule neurons. *J. Neurosci. Res.* 53, 670–676.
- Schacher, S., and Wu, F. (2002). Synapse formation in the absence of cell bodies requires protein synthesis. *J. Neurosci.* 22, 1831–1839.
- Schmidt, E.K., Clavarino, G., Ceppi, M., and Pierre, P. (2009). SUnSET, a nonradioactive method to monitor protein synthesis. *Nat. Methods* 6, 275–277.
- Sheehan, P., Zhu, M., Beskow, A., Vollmer, C., and Waites, C.L. (2016). Activity-dependent degradation of synaptic vesicle proteins requires Rab35 and the ESCRT pathway. *J. Neurosci.* 36, 8668–8686.
- Shigeoka, T., Jung, H., Jung, J., Turner-Bridger, B., Ohk, J., Lin, J.Q., Amieux, P.S., and Holt, C.E. (2016). Dynamic axonal translation in developing and mature visual circuits. *Cell* 166, 181–192.
- Taylor, A.M., Blurton-Jones, M., Rhee, S.W., Cribbs, D.H., Cotman, C.W., and Jeon, N.L. (2005). A microfluidic culture platform for CNS axonal injury, regeneration and transport. *Nat. Methods* 2, 599–605.
- Taylor, A.M., Berchtold, N.C., Perreau, V.M., Tu, C.H., Li Jeon, N., and Cotman, C.W. (2009). Axonal mRNA in uninjured and regenerating cortical mammalian axons. *J. Neurosci.* 29, 4697–4707.
- Taylor, A.M., Wu, J., Tai, H.C., and Schuman, E.M. (2013). Axonal translation of  $\beta$ -catenin regulates synaptic vesicle dynamics. *J. Neurosci.* 33, 5584–5589.
- tom Dieck, S., Kochen, L., Hanus, C., Heumüller, M., Bartnik, I., Nassim-Assir, B., Merk, K., Mosler, T., Garg, S., Bunse, S., et al. (2015). Direct visualization of newly synthesized target proteins in situ. *Nat. Methods* 12, 411–414.
- Tsanov, N., Samacoits, A., Chouaib, R., Traboulsi, A.M., Gostan, T., Weber, C., Zimmer, C., Zibara, K., Walter, T., Peter, M., et al. (2016). smiFISH and FISH-quant - a flexible single RNA detection approach with super-resolution capability. *Nucleic Acids Res.* 44, e165.
- Villarin, J.M., McCurdy, E.P., Martínez, J.C., and Hengst, U. (2016). Local synthesis of dynein cofactors matches retrograde transport to acutely changing demands. *Nat. Commun.* 7, 13865.
- Wu, K.Y., Hengst, U., Cox, L.J., Macosko, E.Z., Jeromin, A., Urquhart, E.R., and Jaffrey, S.R. (2005). Local translation of RhoA regulates growth cone collapse. *Nature* 436, 1020–1024.
- Yarmolinsky, M.B., and Haba, G.L. (1959). Inhibition by puromycin of amino acid incorporation into protein. *Proc. Natl. Acad. Sci. USA* 45, 1721–1729.
- Younts, T.J., Monday, H.R., Dudok, B., Klein, M.E., Jordan, B.A., Katona, I., and Castillo, P.E. (2016). Presynaptic protein synthesis is required for long-term plasticity of GABA release. *Neuron* 92, 479–492.
- Zivraj, K.H., Tung, Y.C., Piper, M., Gumy, L., Fawcett, J.W., Yeo, G.S., and Holt, C.E. (2010). Subcellular profiling reveals distinct and developmentally regulated repertoire of growth cone mRNAs. *J. Neurosci.* 30, 15464–15478.